Polym. Bull. (2012) 68:1153–1169
DOI 10.1007/s00289-011-0671-0

ORIGINAL PAPER

Preparation and characterization of sodium alginate/poly(*N*-isopropylacrylamide)/clay semi-IPN magnetic hydrogels

Zhiqiang Li · Jianfeng Shen · Hongwei Ma · Xin Lu · Min Shi · Na Li · Mingxin Ye

Received: 28 September 2011 / Revised: 10 November 2011 / Accepted: 13 November 2011 /
Published online: 18 November 2011

Abstract pH- and temperature-responsive semi-interpenetrating magnetic nanocomposite hydrogels (NC hydrogels) were prepared by using linear sodium alginate (SA), poly(*N*-isopropylacrylamide) (PNIPAM) and Fe_3O_4 nanoparticles with inorganic clay as an effective multifunctional cross-linker. The effects of cross-linker and SA contents on various physical properties were investigated. The NC hydrogels exhibited a volume phase transition temperature (VPTT) around 32 °C with no significant deviation from the conventional chemically cross-linked PNIPAM hydrogels (OR hydrogels). The swelling ratios of NC hydrogels were much larger than those of OR hydrogels. Moreover, the swelling ratios of NC hydrogels gradually decreased with increasing the contents of clay and increased with increasing the contents of SA. The pH sensitivity of NC hydrogels was evident below their VPTT. The NC hydrogels had a much better mechanical property than the OR hydrogels. The results showed that the incorporation of clay did not affect the saturation magnetization of the hydrogels.

Keywords Hydrogel · Sodium alginate · Poly(*N*-isopropylacrylamide) · Clay · Fe_3O_4 · pH- and temperature-responsive

Introduction

In recent years, stimuli-sensitive hydrogels, a three-dimensional cross-linked polymer network able to change its volume and properties in response to environmental stimuli such as temperature [1], pH [2], solvent composition [3], salt concentration [4], light [5], and magnetic field [6], have attracted great interest.

Z. Li · J. Shen · H. Ma · X. Lu · M. Shi · N. Li · M. Ye (✉)
Center of Special Materials and Technology, Fudan University, 220 Handan Road, Shanghai 200433, China
e-mail: mxye@fudan.edu.cn

Among all the stimuli-sensitive hydrogels, pH- and temperature-responsive hydrogels are most widely investigated because these two factors inside the human body are important [7, 8]. One of the most widely studied temperature-responsive hydrogels is poly(*N*-isopropylacrylamide) (PNIPAM) that has a volume phase transition temperature (VPTT, ~32 °C) in aqueous solution [9, 10]. PNIPAM chains are hydrated to swell at temperatures below the VPTT and become dehydrated to shrink at temperatures above the VPTT. Based on their dramatic swelling and deswelling behaviors, these hydrogels have been used in many fields such as controlled drug delivery [11, 12], chemical separation [13, 14], enzyme immobilization [15], and artificial organ [16].

Sodium alginate (SA) is a particularly attractive material to form hydrogels for biomedical applications [17, 18]. For pH-sensitive hydrogels, SA can be used to form the mainchain because of the carboxyl groups in the SA mainchain. It is a naturally derived linear polysaccharide comprised of β-D-mannuronic acid (M-block) and α-L-guluronic acid (G-block) units arranged in blocks rich in G units or M units, separated by blocks of alternating G and M units. The advantages of using SA for preparing hydrogels also result from the following properties: (1) it has a relatively inert aqueous environment within the matrix, (2) it has a high gel porosity that allows for high diffusion rates of macromolecules, and (3) its dissolution and biodegradation under normal physiological conditions enables it to be used as a matrix for the entrapment and delivery of proteins, drugs and cells [8, 19].

The interpenetrating polymer network (IPN) technology is an effective approach to prepare pH- and temperature-responsive hydrogels [20–22]. IPN is conventionally defined as intimate combination of two polymers, at least one of which is synthesized or cross-linked in the immediate presence of the other [23]. In recent years, semi-IPN gels have attracted particular interest. Lee et al. [24] generated a series of rapidly responsive semi-IPN hydrogels by introducing PNIPAM chains into the alginate networks and chitosan chains. Zhang et al. [25] synthesized a macroporous semi-IPN hydrogels composed of cross-linked PNIPAM and linear SA. However, in these semi-IPN hydrogels, PNIPAM were always cross-linked by an organic cross-linker.

Usually, the PNIPAM hydrogels are prepared by free-radical copolymerization of the monomer (NIPAM) and a chemical organic cross-linker such as *N*,*N*′-methylenebisacrylamide (BIS) [26, 27]. However, the applications of the conventional chemically cross-linked hydrogels (OR hydrogels) are always restricted due to their poor mechanical properties and low response rate [28]. More recently, it was reported that a novel polymer–clay nanocomposite hydrogel (NC hydrogels) was prepared without using any organic cross-linker [29–36]. The incorporation of this clay markedly improves not only the mechanical and swelling-deswelling properties but also the spatial homogeneity of the NC hydrogels. The NC hydrogels were formed by in situ free-radical polymerization, in which the PNIPAM chains were anchored to the surface of clay sheets acting as effective multifunctional cross-linkers through ionic or polar interactions. At the initial stage of polymerization, the initator (APS), which has a divalent anion, was closely associated with the clay surface through ionic interactions and then the propagation reaction was proceeded, thus the polymer chains attach to the clay platelets forming

a network structure. It was also revealed that the unique network could only be formed by free-radical polymerization in the presence of inorganic clay and was not realized by other procedures such as mixing clay and PNIPAM solutions.

From applications' point of view, hydrogels will attract more considerable attention if they could respond to several stimuli simultaneously. The incorporating of metal nanoparticles into the hydrogels has been proved to be an effective approach to enhance the functions of the hydrogels [37]. Magnetite (Fe_3O_4) is one of the important transition metal oxides based on its unique properties including magnetic properties, chemical stability, biocompatibility, and low toxicity. Hydrogels synthesized by embedding Fe_3O_4 nanoparticles inside a polymer network are attractive due to their proven biocompatibility, quick response, and sensitivity to a remotely applied external magnetic field [38]. Therefore, the combination of Fe_3O_4 and hydrogel is expected to constitute a new functional composite with properties of both hydrogel and Fe_3O_4 nanoparticles. To date, there have been no reports on the semi-IPN hydrogels composed of linear SA, PNIPAM, clay and Fe_3O_4 nanoparticles.

In this article, we successfully prepared a novel kind of multifunctional semi-IPN hydrogels based on linear SA, PNIPAM and Fe_3O_4 using inorganic clay as an effective multifunctional cross-linker instead of using the conventional organic cross-linker. We found that because of their unique organic (polymer) and inorganic (clay) network, the NC hydrogels exhibited extraordinary mechanical and swelling/deswelling properties. Compared with the characteristics of OR hydrogels, we presented the characteristics of the NC hydrogels in more detail, focusing on the effects of clay and SA contents.

Materials and methods

Materials

N-isopropylacrylamide (NIPAM), SA, iron(III) acetylacetonate, oleic acid, and oleylamine were purchased from Aldrich. *N*,*N*,*N*′,*N*′-tetramethylethylenediamine (TEMED), ammonium persulfate (APS) and *N*,*N*′-methylenebisacrylamide (BIS) were supplied by Sigma. As an inorganic clay, synthetic hectorite "Laponite XLG" ($[Mg_{5.34}Li_{0.66}Si_8O_{20}(OH)_4]Na_{0.66}$, layer size = 20–30 nm $\Phi \times 1$ nm, cation exchange capacity = 104 mequiv/100 g) was purchased from Rockwood. Absolute ethanol and hexane were used as received.

Preparation of magnetic nanoparticles

Magnetite (Fe_3O_4) nanoparticles covered with oleylamine were prepared by applying a similar method as that in the previous report [39]. $Fe(acac)_3$ (4 mmol), 1,2-hexadecanediol (20 mmol), oleic acid (12 mmol), and phenyl ether (40 mL) were mixed and magnetically stirred under a flow of nitrogen. The mixture solution was heated to 200 °C for 30 min and then, under a blanket of nitrogen, heated to reflux under the same temperature for another 30 min. The dark-brown mixture

solution was cooled to room temperature. Under ambient conditions, ethanol was added to the mixture. The black compound was precipitated and separated with centrifugation. Then the black product was dispersed in hexane.

Preparation of NC hydrogels

The NC hydrogels consist of monomer NIPAM, SA, Fe_3O_4, deionized water and various ratios of clay. In all cases, the initial solution contained 10 times as much water as monomer by weight; the water/polymer ratio in the resulting hydrogels was fixed at 10/1 (w/w). At first, an aqueous solution consisting of water, inorganic clay, SA, NIPAM, and Fe_3O_4 was stirred in ice-water bath for 2 h. Then the catalyst of TEMED (20 μL) was added with stirring. Finally, an aqueous of the initiator APS (0.02 g) was added to the solution. The free-radical polymerization was carried out in a water bath at 20 °C for 24 h. The NC hydrogels are expressed as NCm. The composition for NC hydrogels is shown in Table 1.

The OR hydrogel was also prepared for comparison. In the preparation, 2 wt% BIS based on the monomer NIPAM was used and the contents of other components were the same as those in the NC hydrogels. For the simple identification of the hydrogels, the OR hydrogel is expressed as OR.

Measurement of mechanical properties

Compressive measurements were performed on hydrogels with the same size (10 mm × 10 mm × 10 mm) and the same water/polymer ratio [10/1(w/w)] using a Dejie DXLL-20000. The compression properties of the hydrogels were obtained under the following conditions: test temperature 25 °C, compression speed 0.5 mm/s.

Measurement of swelling ratios

The swelling ratios of hydrogel samples were measured in the temperature range from 20 to 50 °C or in a pH range from 1.2 to 9.0 using a gravimetric method.

Table 1 Preparation condition and swelling properties of NC hydrogels

Sample	NIPAM (g)	SA (g)	Clay (g)	BIS (g)	Fe_3O_4 (g)	SW_{eq}
NC1	1.000	0.050	0.200	0	0.100	66.34
NC2	1.000	0.050	0.400	0	0.100	58.10
NC3	1.000	0.050	0.600	0	0.100	38.57
NC4	1.000	0.050	0.800	0	0.100	30.58
NC5	1.000	0.050	1.000	0	0.100	25.55
NC6	1.000	0.100	0.400	0	0.100	62.50
NC7	1.000	0.200	0.400	0	0.100	70.02
NC0	1.000	0	0.400	0	0.100	40.91
OR	1.000	0.050	0	0.020	0.100	22.62

Under each particular condition, hydrogel samples were incubated in the medium for at least 48 h and removed, wiped with moistened filter paper to remove water from the sample surfaces, and weighed. The swelling ratio was calculated with the following equation:

$$\text{Swelling ratio} = (W_s - W_d)/W_d,$$

where W_s is the weight of the swollen hydrogel, and W_d is the weight of the dry hydrogel.

Deswelling behavior of hydrogels

The deswelling behavior of the hydrogel was studied by recording the weight of water in the hydrogels. Water retention was calculated as

$$\text{Water retention} = (W_t - W_d)/(W_s - W_d),$$

where W_t is the weight of the hydrogel at a given time interval during the course of deswelling after the swollen hydrogel at 25 °C had been quickly transferred into hot water at 45 °C.

Magnetic measurements

Magnetization curves for the NC2 and OR hydrogels were measured by using a vibrating sample magnetometer (MPMS (SQUID) VSM, Quantum Design) with a maximum magnetic field of 7 T, sensibility of 10^{-8} emu. To determine the coercivity, samples were firstly cooled in a zero-applied magnetic field, from room temperature down to the measuring temperature. Dry NC2 and OR hydrogels were fixed on quartz holders, which were placed in the magnetometer. Magnetization results of the hydrogels were determined by applying an increasing magnetic field at 273 K.

Characterizations

Fourier transform infrared spectroscopy (FTIR) spectra were recorded on a NEXUS 670 spectrometer. X-ray diffraction (XRD) patterns were obtained with Cu Kα X-rays performed on a D/max-γB X-ray diffractometer (40 kV, 30 mA) in a step of 0.02°/s from 2° to 70°. The morphology of the fractured specimens was observed on a SUPERSCAN SSX-550 scanning electron microscopy (SEM) at 20 kV after sputter coating with gold under vacuum. The size and morphology of the magnetic nanoparticles were observed by a Hitachi H600 TEM. The VPTT measurements of the wet samples were carried out on a TAQ100 differential scanning calorimeter (DSC) under a nitrogen atmosphere, at a heating rate of 3 °C/min from 20 to 50 °C. Thermogravimetric (TG) analyses were conducted with Netzsch TG 209F1, heating samples from ambient temperature to 700 °C at the heating rate of 20 °C/min in an nitrogen atmosphere.

Results and discussion

Scheme 1 describes the formation process of the NC hydrogels via situ free-radical polymerization in the presence of SA, NIPAM, and Fe_3O_4 with clay as a cross-linker. It is considered that the initator APS could strongly interact with clay platelets through ionic interactions and their molecules were closely associated on the clay surface in aqueous suspension. At the initial stage of polymerization, radical existed near the clay surface, and then the propagation reaction was proceed, thus the PNIPAM chains attached to the clay platelets forming a network structure. In order to confirm whether SA was also cross-linked by clay or existed in a form of linear chains, a mixture of the aqueous solution of clay and SA with the same composition was prepared and remained in water bath at 20 °C for 24 h. It was seen that a turbid gel-like material was formed. However, when further immersed in an excess of water, it turned to be a turbid solution. Therefore, it could be inferred that SA was not cross-linked by clay and still as linear chains incorporated in the hydrogels just like that in the conventional OR hydrogel.

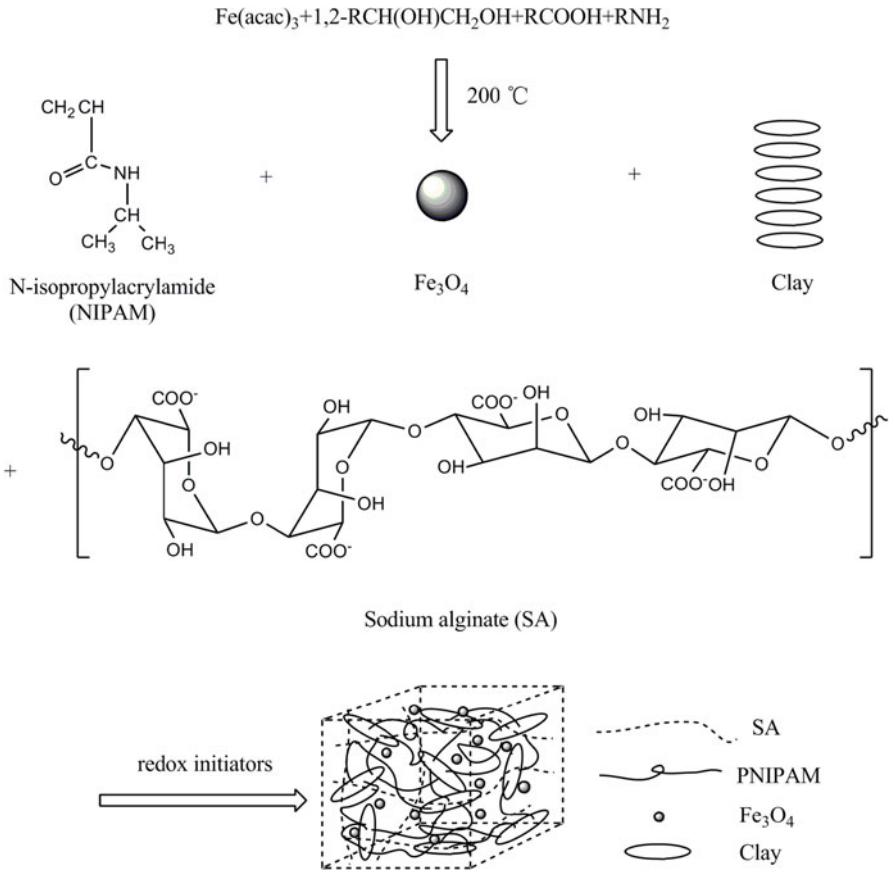

Scheme 1 The formation process of NC hydrogels

FTIR study

The FTIR spectra of the SA, NIPAM, clay, Fe_3O_4 and the dried NC2 are shown in Fig. 1. A band at 1,015 cm^{-1} attributed to a Si–O stretching vibration can be found in the spectrum of the clay. From the spectrum of NIPAM, there is a carbonyl stretching vibration (amide I) at 1,660 cm^{-1}, N–H bending vibration (amide II) at 1,547 cm^{-1} and two typical peaks of C–H vibrations of $-CH(CH_3)_2$. The spectrum of SA shows the characteristic absorption peak of SA units at $\sim$1,662 cm^{-1} due to carboxylate anion of SA groups. In the spectrum of oleic acid modified Fe_3O_4 nanoparticles, the Fe–O bonds appeared at 584 cm^{-1}. As a result, it can be concluded that all the components used to form the semi-IPN hydrogel are present.

X-ray diffraction

The XRD patterns of clay, Fe_3O_4, OR, and NC hydrogels were shown in Fig. 2. Figure 2a can reveal the level of dispersion of clay platelets in the hydrogels. It is clearly seen that almost no distinct diffraction peak at around for 2θ in the range 2°–10° was observed for NC1 and NC5 hydrogels, while the clay showed a diffraction peak at $2\theta = 5.94°$, corresponding to a basel spacing of 1.49 nm between clay sheets. This indicates that clay was sufficiently exfoliated in the dried hydrogels. Therefore, it was considered that exfoliated clay was uniformly dispersed in the NC hydrogels, which was largely expanded with water. Also, from the XRD patterns of Fe_3O_4 and NC samples, six characteristic peaks for Fe_3O_4 ($2\theta = 30°$, 36°, 43°, 54°, 58°, and 63°) were observed in both the samples. These peaks are consistent with the findings of other groups [40], indicating the presence of Fe_3O_4, thus verifying the existence of magnetite within the composite hydrogels.

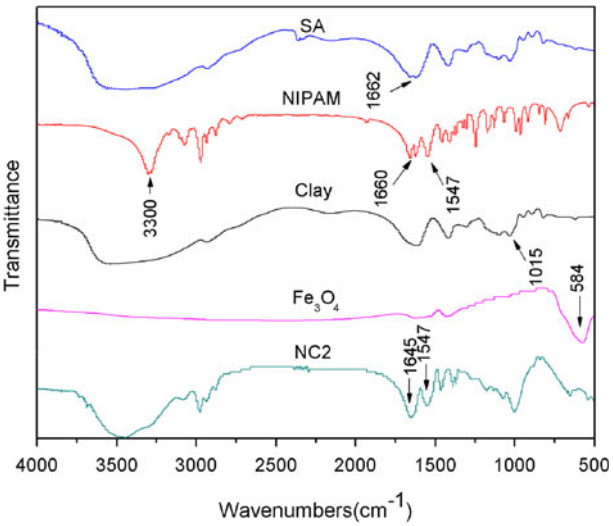

Fig. 1 FTIR spectra of SA, NIPAM, Clay, Fe_3O_4 and NC2 hydrogel

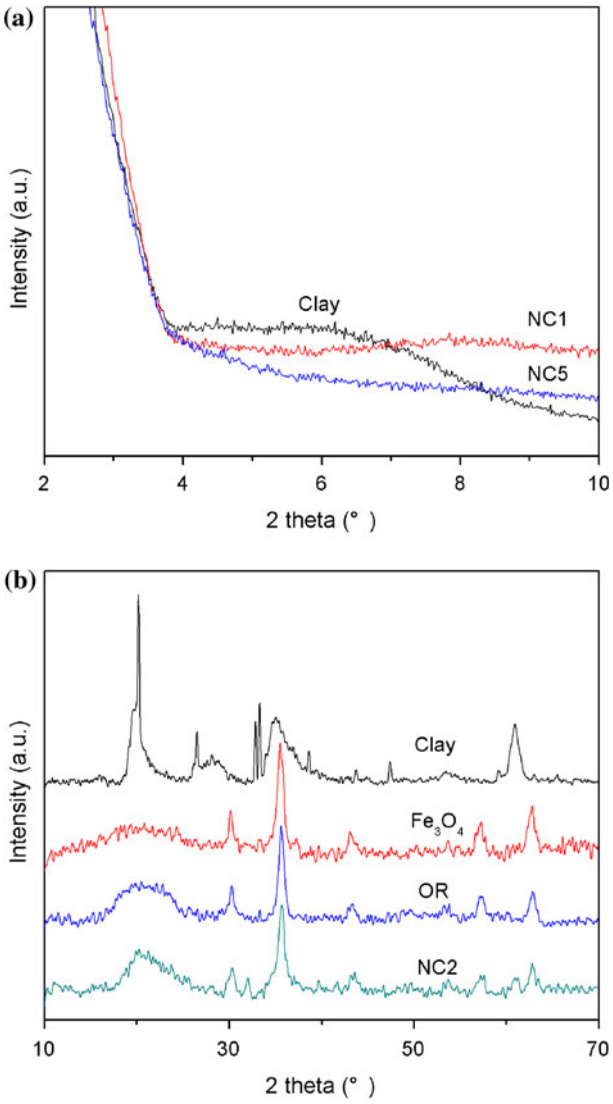

Fig. 2 XRD patterns of Clay, Fe_3O_4, OR and NC hydrogels

VPTT of the hydrogels

The DSC thermograms of OR and NC hydrogels are shown in Fig. 3. The temperature at the onset point of the DSC endotherm is referred to the VPTT of the hydrogels [41]. At the VPTT, the water in the hydrogels will be separated from the network, leading to a smaller heat capacity. As shown in Fig. 3, the OR hydrogel and NC hydrogels exhibited a similar VPTT around 32 °C, and there is no significant deviation from the VPTT of the OR hydrogel. The results indicate that in

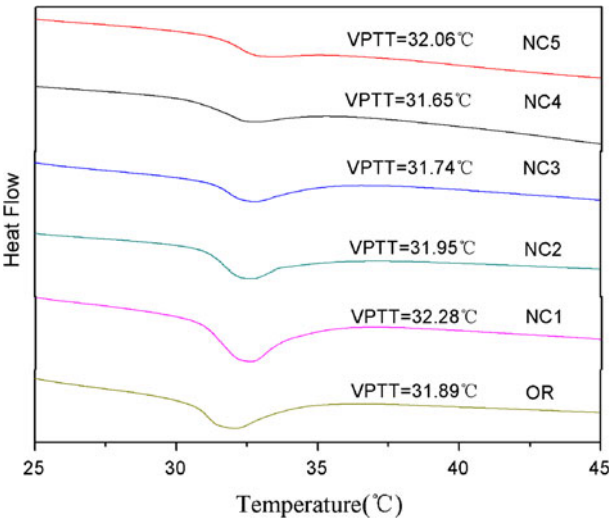

Fig. 3 DSC thermograms of OR and NC hydrogels

the semi-IPN system, the PNIPAM network retains its own property because there is no chemical bond between SA and PNIPAM network. On the other hand, it can also be concluded that the VPTT of the hydrogel network is independent of the type and content of the cross-linker used in this study. This is agreed with the findings of other groups [30, 42, 43]. Also, the incorporation of the Fe_3O_4 nanoparticles has no effects on the VPTT of the hydrogels.

Morphological studies

When samples are freeze dried, movement of polymer chains is highly restricted since the entire sample is in the solid state (both polymer chains and water molecules). Thus, as water molecules are removed by sublimation, the polymer chains cannot move and remain in the same conformation [44].

The morphological characteristics of NC hydrogels after exposure to solutions and subsequent freeze drying have been examined by SEM. Figure 4 show the SEM micrographs of the internal structure of NC hydrogels, from which we can see that the semi-IPN hydrogels show a porous network structure in character. These results showed that a highly expanded network can be generated by electrostatic repulsions among SA carboxylate anions (–COO–) during the polymerization process. Therefore, the response rate could greatly be enhanced by the incorporation SA into the hydrogels network during the deswelling process. Also, with increasing clay content, the cross-link densities of the hydrogels increased, resulting in the decrease in the pore size. When the temperature is above the hydrogel's VPTT, the water molecules are hard to diffuse out as a result of numerous small pores in the hydrogel network. So the swelling ratio decreased with increasing the contents of clay [30].

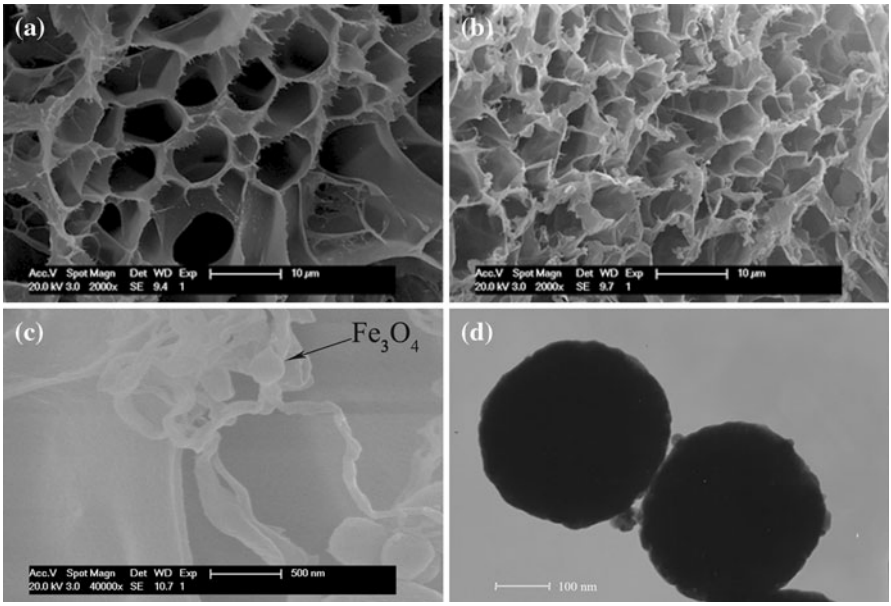

Fig. 4 SEM and TEM images of NC1 (**a**), NC5 (**b**), NC1 (**c**), Fe_3O_4 (**d**)

Also, the TEM images of Fe_3O_4, shown in Fig. 4d, revealed that the Fe_3O_4 particles display their spherical shape and have a good dispersion. Figure 4c shows that the magnetite particles were distributed evenly over the whole area of hydrogels.

Thermogravimetric analysis

Figure 5 illustrates the thermograms of the hydrogels and Fe_3O_4. According to the TGA results, the Fe_3O_4 particles have no significant weight change, and the NC hydrogels showed a higher thermal stability compared with the OR hydrogel. Also, the NC hydrogels showed a higher thermal stability with increasing the contents of the clay. It could be due to the higher physical cross-linking within the networks, which may results from the clay content.

Mechanical properties of hydrogels

The compressive stress–strain curves (up to 100% compression) of NC hydrogels and OR hydrogel were shown in Fig. 6. Here, it should be noted that all NC and OR hydrogels used for mechanical tests have same size (5.5 mm $\Phi \times$ 70 mm length) and the same water/polymer ratio (10/1 (w/w)). The hydrogels prepared by two types of the cross-linkers exhibited completely different mechanical properties. As described previously, the OR hydrogel was so weak and brittle that it could not be applied in many fields. Here, the OR hydrogel fractured at a low strain (61%) and

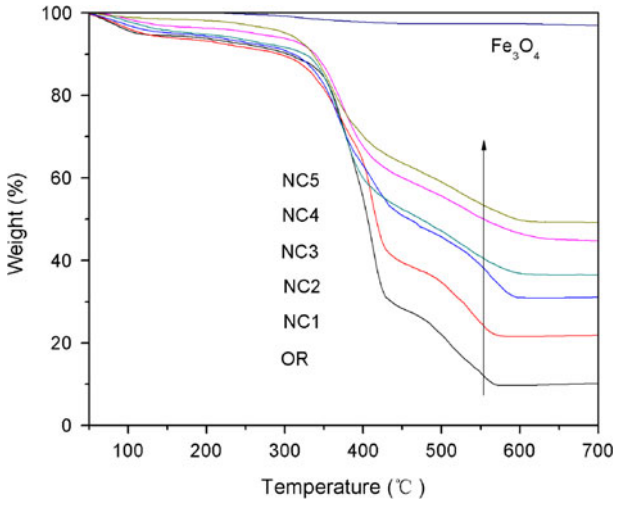

Fig. 5 TGA thermograms of the hydrogels and Fe_3O_4

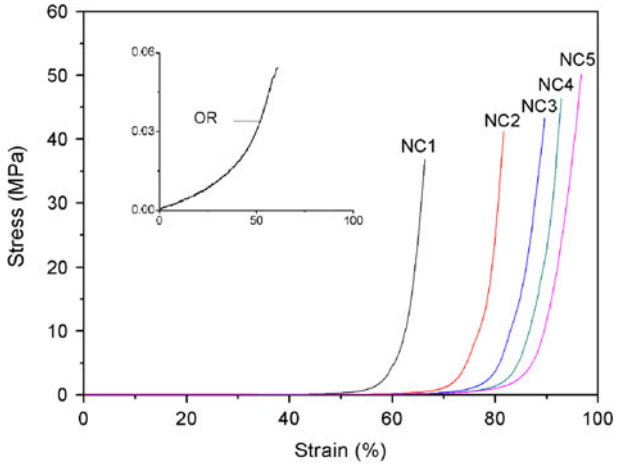

Fig. 6 Compressive stress–strain curves of OR and NC hydrogels

had a low compressive strength (0.2 MPa). On the contrary, the NC hydrogels generally exhibited very high strain and rigidity. Also, it was observed that the mechanical properties of NC hydrogels strongly depend on the contents of clay. The mechanical properties of NC hydrogels increased with increasing the contents of clay. As mentioned above, the average intercross-linked distances in the NC hydrogels network were larger than those in the OR hydrogel. The PNIPAM chains in the swollen state could be regarded as flexible polymer chains just like those in the rubbery state and thus the large deformation could be realized.

Temperature dependence of the hydrogels

The swelling ratios of NC and OR hydrogels were investigated as a function of temperature at pH 1.2 and 7.4, respectively, as shown in Fig. 7. In general, an abrupt decrease of the swelling ratios can be observed around VPTT for the samples, which is ascribed to the coil-globular transition of PNIPAM. At pH 7.4 and temperature below the VPTT, the swelling ratios of OR hydrogel are lower than those of NC hydrogels. It was theoretically evaluated by Haraguchi [29] that the polymer chain between the cross-linking points in hydrogels cross-linked by clay were long and flexible, and the distribution of chain lengths was fairly narrow. Therefore, it is reasonable to infer that the hydrogels cross-linked by clay have lower cross-link density than those of OR hydrogels cross-linked by BIS. Among NC hydrogels, the swelling ratios of NC hydrogels gradually decrease with increasing the contents of

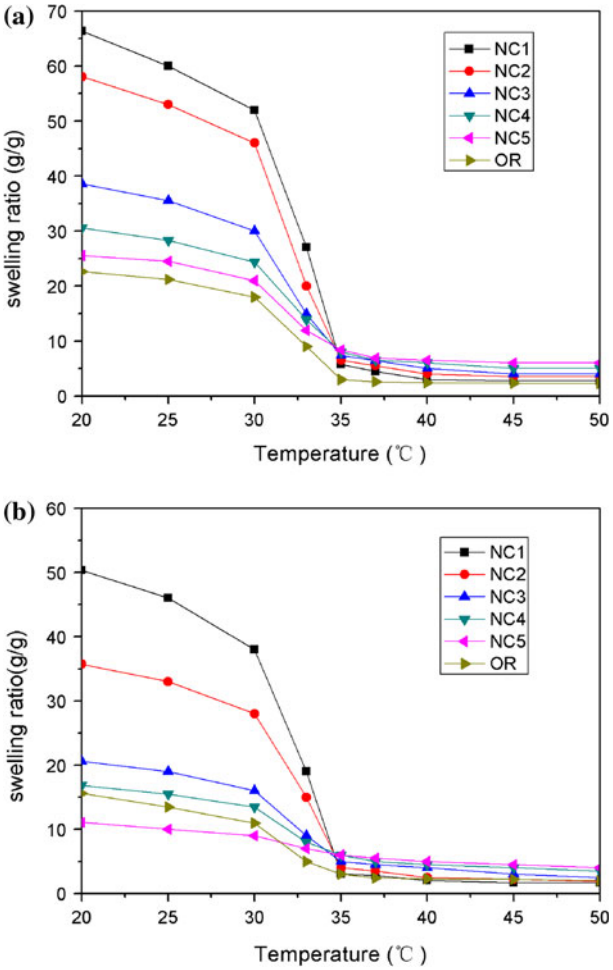

Fig. 7 Swelling ratios of OR and NC hydrogels as a function of temperature at pH 7.4 (**a**) and pH 1.2 (**b**)

clay. As mentioned above, the inorganic clay platelets acted as multifunctional cross-linkers with PNIPAM chains linked on them. The NC hydrogels with higher clay contents leaded to form more densely cross-linked networks, and thus decreased the swelling ratios of the hydrogels [30, 43]. By comparing Fig. 7a and b, it can also be found that the swelling ratios of the hydrogels below VPTT at pH 1.2 are lower than those at pH 7.4. This phenomenon may be due to the fact that most of –COO– groups in SA are protonated under acidic conditions, thus forming hydrogen bond between –COOH and –CONH– groups, which lead to the polymer–polymer interactions predominating over the polymer–water interactions.

pH dependence of the hydrogels

Sodium alginate is a kind of natural polyelectrolyte, which has many carboxylic groups in its molecular chain, the pKa of SA is about 3.2 and 4.0 for guluronic and mannuronic acids, respectively. To investigate the influence of pH value of the medium on the swelling ratios for the NC hydrogels, the pH range is selected from 1.2 to 9.0 in this study. As shown in Fig. 8, the swelling ratios of NC hydrogels with various SA contents are lower than those of pure PNIPAM hydrogel in the pH value range from 1.2 to 2. It is due to the formation of hydrogen bond between –COOH in the SA and –CONH– in the PNIPAM and, thus, leading to polymer–polymer interactions predominating over the polymer–water interactions, which results in a decrease of swelling ratios. Furthermore, that is, under strong acidic conditions, the higher the SA contents in the NC hydrogels, and the lower the swelling ratios of the NC hydrogels. In the pH range from 1.2 to 6.4, the swelling ratios of the semi-IPN hydrogels continuously increase with increasing pH values. As the pH value of the medium increases, the carboxylic acid groups become ionized and the electrostatic repulsion between the molecular chains is predominated which leads to the network

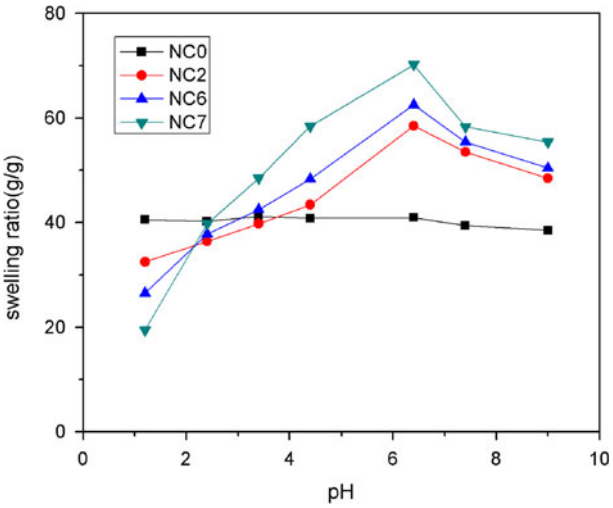

Fig. 8 Swelling ratios of NC hydrogels as a function of pH value of the medium at 25 °C

more expanding. At pH 6.4, there is a maximum swelling ratio for the NC hydrogels. Beyond this value, a screening effect of the counter ions, i.e., Na^+, shielding the charge of the carboxylate anions may prevents from an efficient repulsion. As a result, a remarkable decrease in equilibrium swelling is observed. As a contrast, for the pure PNIPAM gel, the swelling ratios keep constant when pH changes in the range studied above.

Deswelling kinetics

As mentioned above, the deswelling rate is one of the most important factors and, in particular, high rates are needed in many applications. A general approach to high swelling rate is to utilize the size effect. Hydrogels with smaller size could exhibit higher deswelling rates because of the smallest dimension of the gel. Here, all initial samples started with the same volume (712 mm^3) and the same water/polymer ratio (10/1 (w/w)). Figure 9 shows the deswelling behaviors measured for NC hydrogels containing different clay contents under the same experimental conditions. Contrary to OR hydrogel, the NC hydrogels containing lowest clay content exhibited the most rapid response. Furthermore, the deswelling rate gradually decreased as the contents of clay increased. It should be noted that the NC hydrogels with low contents of clay have much higher response rates than the OR hydrogel. For instance, NC1 hydrogel loses about 80% water within 80 min, whereas the OR hydrogel takes 5 h to lose only 60% water.

Magnetization

Magnetization curves of OR and NC2 hydrogels recorded with VSM are illustrated in Fig. 10. No remanence nor coercivity were observed for each sample, indicating that the Fe_3O_4 nanoparticles embedded in the supromolecular hydrogel are

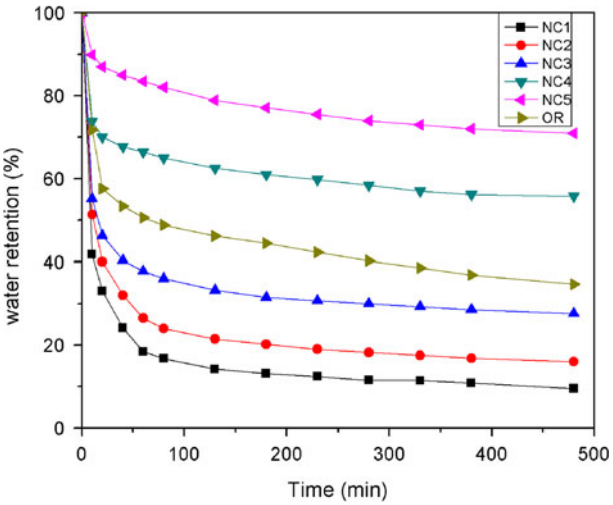

Fig. 9 Deswelling behavior of OR and NC hydrogels at 45 °C (pH 7.4)

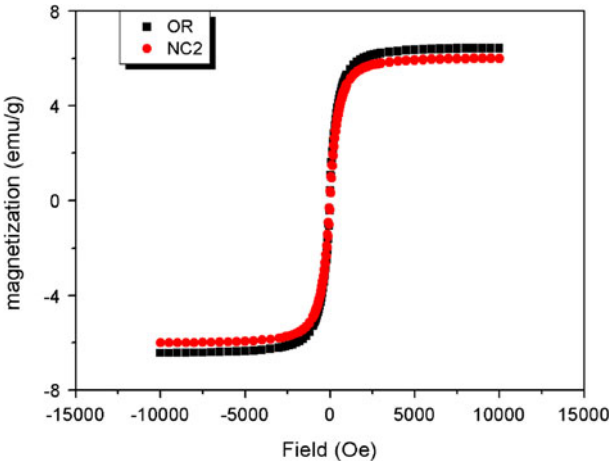

Fig. 10 Magnetization curves of OR and NC2 hydrogels

superparamagnetic and the single-domain magnetite nanoparticles remained in the polymer network [44, 45]. Superparamagnetism, that is, responsiveness to an applied magnetic field without permanent magnetization, is an especially important property needed for magnetic bioseparation because it ensures repeated use of magnetic adsorbents and efficient product elution. In addition, the saturation magnetization was found to be 6.24 emu/g for OR hydrogel and 6.04 emu/g for NC2 hydrogel. The results of saturation magnetization showed that the incorporation of clay in the NC hydrogels did not affect the saturation magnetization of the hydrogels.

Conclusions

In this article, pH- and temperature-responsive semi-IPN magnetic hydrogels were prepared by introducing Fe_3O_4 into the PNIPAM and SA hydrogels network, which was cross-linked by inorganic clay acting as a multifunctional cross-linker. The novel NC hydrogels exhibit the same VPTT around 32 °C as that of the conventional OR hydrogels. The swelling ratios of NC hydrogels below VPTT are much larger than those of OR hydrogels. Moreover, the swelling ratios of NC hydrogels gradually decreased with increasing the contents of clay and increased with increasing the contents of SA. The pH sensitivity of NC hydrogels was evident below their VPTT. Also, the NC hydrogels have a much better mechanical property than that of the OR hydrogel. The results showed that the incorporation of clay did not affect the saturation magnetization of the hydrogels.

References

1. Kiler J, Scranton AB, Peppas NA (1990) Self-associating networks of poly(methacrylic acid-g-ethylene glycol). Macromolecules 23(23):4944–4949

2. Chiu HC, Lin YF, Hung SH (2002) Equilibrium swelling of copolymerized acrylic acid-methacrylated dextran networks: effects of pH and neutral salt. Macromolecules 35(13):5235–5242
3. Kokufata E, Zhang YQ, Tanaka T (1991) Saccharide-sensitive phase transition of a lectin-loaded gel. Nature 351:302–304
4. Dhara D, Chatterji PR (2000) Swelling and deswelling pathways in nonionic poly(*N*-isopropylacrylamide) hydrogels in presence of additives. Polymer 41(16):6133–6143
5. Suzuki A, Tanaka T (1990) Phase transition in polymer gels induced by visible light. Nature 346:345–347
6. Xulu PM, Filipcsei G, Zrinyi M (2000) Preparation and responsive properties of magnetically soft poly(*N*-isopropylacrylamide) gels. Macromolecules 33(5):1716–1719
7. Serizawa T, Wakita K, Akashi M (2002) Rapid deswelling of porous poly(*N*-isopropylacrylamide) hydrogels prepared by incorporation of silica particles. Macromolecules 35(1):10–12
8. Kim JH, Lee SB, Kim SJ, Lee YM (2002) Rapid temperature/pH response of porous alginate-g-poly(*N*-isopropylacrylamide) hydrogels. Polymer 43(26):7549–7558
9. Tanaka Y, Kagami Y, Matsuda A, Osada Y (1995) Thermoreversible transition of tensile modulus of hydrogel with ordered aggregates. Macromolecules 28(7):2574–2576
10. Zhang J, Peppas NA (2002) Morphology of poly(methacrylic acid)/poly(*N*-isopropylacrylamide) interpenetrating polymeric networks. J Biomater Sci Polym Ed 13(5):511–525
11. Tang YF, Zhao YY, Li Y, Du YM (2010) A thermosensitive chitosan/poly(vinyl alcohol) hydrogel containing nanoparticles for drug delivery. Polym Bull 64(8):791–804
12. Hoffman AS (2002) Hydrogels for biomedical applications. Adv Drug Rev 54(1):3–12
13. Kawaguchi H, Fujimoto K (1998) Smart latexes for bioseparation. Bioseparation 7(4/5):253–258
14. Zhang QS, Li XW, Zhao YP, Chen L (2009) Preparation and performance of nanocomposite hydrogels based on different clay. Appl Clay Sci 46(4):346–350
15. Liu F, Tao GL, Zhuo RX (1993) Synthesis of thermal phase separating reactive polymers and their applications in immobilized enzymes. Polym J 25(6):561–567
16. Shiino D, Murata Y, Kataoka K, Koyama Y, Yokoyama M, Okano T, Sakurai Y (1994) Preparation and characterization of a glucose-responsive insulin-releasing polymer device. Biomaterials 15(2):121–128
17. Miyazaki S, Nakayama A, Oda M, Takada M, Attwood D (1995) Drug release from oral mucosal adhesive tablets of chitosan and sodium alginate. Int J Pharm 118(2):257–263
18. Wang CY, Liu HX, Gao QX, Liu XX, Tong Z (2008) Alginate-calcium carbonate porous microparticle hybrid hydrogels with versatile drug loading capabilities and variable mechanical strengths. Carbohydr Polym 71:476–480
19. Zhang GQ, Zha LS, Zhou MH, Ma JH, Liang BR (2005) Preparation and characterization of pH- and temperature-responsive semi-interpenetrating polymer network hydrogels based on linear sodium alginate and crosslinked poly(*N*-isopropylacrylamide). J Appl Polym Sci 97(5):1931–1940
20. Guo BL, Gao QY (2007) Preparation and properties of a pH/temperature-responsive carboxymethyl chitosan/poly(*N*-isopropylacrylamide) semi-IPN hydrogel for oral delivery of drugs. Carbohydr Res 342(16):2416–2422
21. Zhao SP, Li YL, Cao MJ, Xu WL (2011) pH- and thermo-sensitive semi-IPN hydrogels composed of chitosan, *N*-isopropylacrylamide, and poly(ethylene glycol)-co-poly(ε-caprolactone) macromer for drug delivery. Polym Bull 66(8):1075–1087
22. Zhang GQ, Zha LS, Zhou MH, Ma JH, Liang BR (2005) Rapid deswelling of sodium alginate/poly(*N*-isopropylacrylamide) semi-interpenetrating polymer network hydrogels in response to temperature and pH changes. Colloid Polym Sci 283(4):431–438
23. Bajpai AK, Bajpai J, Shukla S, Kulkarni RA (2004) Modulation in sorption dynamics of a pH-sensitive interpenetrating polymer network (IPN). J Marcromol Sci A 41(2):211–230
24. Lee WF, Chen YJ (2001) Studies on Preparation and swelling properties of the *N*-isopropylacrylamide/chitosan semi-IPN and IPN hydrogels. J Appl Polym Sci 82(10):2487–2496
25. Zhang JT, Cheng SX, Zhuo RX (2003) Poly(vinyl alcohol)/poly(*N*-isopropylacrylamide) semi-interpenetrating polymer network hydrogels with rapid response to temperature changes. Colloid Polym Sci 281(6):580–583
26. Sayil C, Okay O (2000) The effect of preparation temperature on the swelling behavior of poly(*N*-isopropylacrylamide) gels. Polym Bull 45(2):175–182
27. Sayil C, Okay O (2002) Macroporous poly(*N*-isopropylacrylamide) networks. Polym Bull 48(6):499–506

28. Shibayama M, Morimoto M, Nomura S (1994) Phase separation induced mechanical transition of poly(*N*-isopropylacrylamide)/water isochore gels. Macromolecules 27(16):5060–5066
29. Haraguchi K, Takehisa T (2002) Nanocomposite hydrogels: a unique organic- inorganic network structure with extraordinary mechanical, optical, and swelling/deswelling properties. Adv Mater 14(16):1120–1124
30. Haraguchi K, Takehisa T, Fan S (2002) Effects of clay content on the properties of nanocomposite hydrogels composed of poly(*N*-isopropylacrylamide) and clay. Macromolecules 35(27):10162–10171
31. Shibayama M, Suda J, Karino T, Okabe S, Takehisa T, Haraguchi K (2004) Structure and dynamics of poly(*N*-isopropylacrylamide)-clay nanocomposite gels. Macromolecules 37(25):9606–9612
32. Haraguchi K, Li HJ, Matsuda K, Takehisa T, Elliott E (2005) Mechanism of forming organic/inorganic network structures during in situ free-radical polymerization in PNIPA-clay nanocomposite hydrogels. Macromolecules 38(8):3482–3490
33. Haraguchi K, Takada T (2005) Characteristic sliding frictional behavior on the surface of nanocomposite hydrogels consisting of organic-inorganic network structure. Macromol Chem Phys 206(15):1530–1540
34. Hu XB, Wang T, Xiong LJ, Wang CY, Liu XX, Tong Z (2010) Preferential adsorption of poly(ethylene glycol) on hectorite clay and effects on poly(*N*-isopropylacrylamide)/hectorite nanocomposite hydrogels. Langmuir 26(6):4233–4238
35. Wang T, Liu D, Lian CX, Zheng SD, Liu XX, Wang CY, Tong Z (2011) Rapid cell sheet detachment from alginate semi-interpenetrating nanocomposite hydrogels of PNIPAm and hectorite clay. React Funct Polym 71:447–454
36. Xiong LJ, Zhu MN, Hu XB, Liu XX, Tong Z (2009) Ultrahigh deformability and transparence of hectorite clay nanocomposite hydrogels with nimble pH response. Macromolecules 42:3811–3817
37. Mayer CR, Cabuil V, Lalot T, Thouvenot R (1999) Incorporation of magnetic nanoparticles in new hybrid networks based on heteropolyanions and polyacrylamide. Angew Chem Int Ed 38(24):3672–3675
38. Paulino AT, Guilherme MR, de Almeida EAMS, Pereira AGB, Muniz EC, Tambourgi EB (2009) One-pot synthesis of a chitosan-based hydrogel as a potential device for magnetic biomaterial. J Magn Magn Mater 321(17):2636–2642
39. Sun SH, Zeng H, Robinson DB, Raoux S, Rice PM, Wang SX, Li GX (2004) Monodisperse MFe_2O_4 (M = Fe, Co, Mn) nanoparticles. J Am Chem Soc 126(1):273–279
40. Li P, Zhu AM, Liu QL, Zhang QG (2008) Fe_3O_4/poly(*N*-isopropylacrylamide)/chitosan composite microspheres with multiresponsive properties. Ind Eng Chem Res 47(20):7700–7706
41. Otake K, Inomata H, Konno M, Saito S (1990) Thermal analysis of the volume phase transition with *N*-isopropylacrylamide gels. Macromolecules 23(1):283–289
42. Ma JH, Xu YJ, Zhang QS, Zha LS, Liang BR (2007) Preparation and characterization of pH- and temperature-responsive semi-IPN hydrogels of carboxymethyl chitosan with poly(*N*-isopropylacrylamide) crosslinked by clay. Colloid Polym Sci 285(4):479–484
43. Ma JH, Xu YJ, Fan B, Liang BR (2007) Preparation and characterization of sodium carboxymethylcellulose/poly(*N*-isopropylacrylamide)/clay semi-IPN nanocomposite hydrogels. Eur Polym J 43(6):2221–2228
44. Liang YY, Zhang LM, Li W, Chen RF (2007) Polysaccharide-modified iron oxide nanoparticles as an effective magnetic affinity adsorbent for bovine serum albumin. Colloid Polym Sci 285(11):1193–1199
45. Ma ZY, Guan YP, Liu HZ (2005) Synthesis and characterization of micron-sized monodisperse superparamagnetic polymer particles with amino groups. J Polym Sci A 43(15):3433–3439